

Using the Finite Element Analysis of Digitalized Photos to Evaluate the Quality of Concrete

Ragab M. Abd El-Naby, Emad A. M. El-Dardiryand Naji A. Abo Azzom

Civil Engineering Department, Faculty of Engineering at Shoubra, Benha University
e_eldardiry@yahoo.co.uk, emad.eldardiry@feng.bu.edu.eg

Abstract: The characterization of concrete on macrostructure based evaluation using the numerical techniques is still limited because modeling the concrete as a single-phase material. Therefore, misunderstanding the actual behavior of the concrete elements is the end result. On the other hand, microstructural analysis are still qualitative technique and very difficult to be used to assess the mechanical characteristics of the concrete. The foregoing difficulties motivated researchers to seek new concepts to maximize the benefits from using the finite element analysis. The Digital Image Analysis has been used to identify aggregate quality and gradation. Recently, attempts are carried out to relate the output of the digital image processing to the numerical analysis. Concrete cylindrical specimens of different mixes that manually or mechanically compacted were used to implement the experimental program. The concrete specimens were saw cut and photographed using digital camera. The photos were treated using computer software to be transferred to the AUTOCAD program as two layers; cement mortar and aggregate. Then, the AUTOCAD files were exported to the finite element analysis software SAP2000 to verify the influence of the aggregate type and the method of compaction on the quality and the mechanical properties of the concrete mixes. The results showed that linking the output data of the digital image processing to the finite element analysis led to identify the concrete as a multiphase layers system and consequently, the finite element program succeeded to predict the location of failure inside the system (in the cement mortar, the aggregate, or at the interface). Also, the finite element analysis succeeded to distinguish among concrete mixes that contained gravel or dolomite aggregates which were compacted using manual or mechanical compaction.

[Ragab M. Abd El-Naby, Emad A. M. El-Dardiryand Naji A. Abo Azzom. **Using the Finite Element Analysis of Digitalized Photos to Evaluate the Quality of Concrete.** *J Am Sci* 2013;9(12):489-505]. (ISSN: 1545-1003). <http://www.americanscience.org>. 66

Keywords: Single phase material, Double phase material, Cement mortar, Interface, Failure, Digital image analysis.

1. Introduction

Modeling the concrete as a single-phase material in the finite element analysis will not lead to understand the actual behavior of the structure of mixes(1,2). So, researchers are seeking for an approach to identify the composite material as coarse aggregate immersed randomly in the cement mortar (3,4). The Digital Image Analysis (DIA) is usually used to implement qualitative and quantitative evaluation (5,6). It is believed that the DIA can be an effective technique to express the concrete as a double-phase material (7,8). Relating the DIA output to the finite element analysis seems to be the required approach and should be verified (9, 10). The combined method should consider the following:

- 1-The combined method can easily and thoroughly explain the mechanisms of failure of the concrete.
- 2-The method should easily relate the microstructure characteristics to the mechanical properties of the concrete.
- 3-The method should be easily implemented and should not need special equipment difficult to interpret.

2. Objectives

The presented research work aims to seek the following:

- 1- Finding the method of linking the results of the digital image processing to the finite element program.
- 2- Using the combined method to verifying the role of aggregate type and compaction method on the concrete compressive strength.
- 3- Using the finite element to find the most probable place of failure inside the concrete wherever inside the aggregate, the mortar, or at the interface.

3. Materials characterization and modeling:

The experimental and analytical programs were implemented using 24 concrete cylinders of 100mm diameter and 200mm long which were casted and cured in water for 28 days. Sixteen cylinders were kept for implementing the compression and indirect tension tests and eight cylinders were used to carry out the DIA. Photos from (1) to (3) and Figure (1) show the implemented experimental and analytical programs. The compressive and tensile strengths are presented in Table (1).

Four concrete cylinders which contained gravel were divided into two groups. The concrete cylinders in the first group were manually compacted while in the second group they were mechanically compacted. The first cylinder in each group was saw cut longitudinally through the axis passing the center of

the cylinder and it was photographed using digital camera of high resolution set at a fixed distance of 1.0m. Photo (1) and Figure (1) explains the experimental procedure. The second cylinder in each group was saw-cut horizontally at top (20mm from top surface) and mid-sections as shown in Photo (2). The cross sections were photographed as explained above. The image was converted from color image to white and black image. The specimen was cut out from the whole image using a program called "Photo Effect", and then it was saved in "TIFF" extension. The image was analyzed by a new software called "VEXTRACTOR DEMO" version 5 to convert the image from "JPG" to "DXF" to treat it as AUTOCAD drawing. The Digital image processing was similarly implemented on the other four cylinders which contained dolomite. The finite element analysis was carried out on four vertical sections and eight horizontal sections.

The shell element used in modeling the specimens was defined as full shell elements. The Material properties were linear elastic and isotropic. The isotropic mechanical and thermal properties relating strain to stress and temperature change were as follows:

E1 : Young's modulus of elasticity,

μ 12: Poisson's ratio,

G1 : Shear modulus, and

α 1 : Coefficient of thermal expansion.

This relationship holds regardless of the orientation of the Material local axes 1, 2, and 3. Table (2) summarizes the values of the specified characteristics used in the finite element program. The specimens were modified in AUTOCAD by drawing a 3D-face element in the bottom left corner in a layer nominated "cement mortar" and arrayed to the whole image. Internal 3D-face element has been stretched to the perimeter of the aggregate and converted to a new layer nominated "aggregate". The drawing was saved in "DXF" extension and imported in SAP 2000 in two steps. In the first step, the "aggregate" layer was imported and defined as shown in Table (1). After that, the "cement paste" layer was imported and defined as given in Table (1). The reference specimen was modeled using shell element. The specimen is divided into 3200 elements of dimensions (2.5mm \times 2.5mm).

4. Failure criterion and definitions:

The concrete was considered ultimately failed if the induced tensile stress is more than 30kg/cm². It is assumed that full bond at the interface between the aggregate and the cement paste is existed. Two levels of comparison are made based on the induced normal stress S11. The normal stress S11 is defined as the normal stress induced in the direction perpendicular to the direction of the applied load. The compressive and

tensile strength results are shown in Table (1). The compressive strength of manually compacted concrete specimens contained gravel is taken as reference to calculate the load of each node as follows:

$$\text{Compressive load} = f_{cu} (\text{kg/cm}^2) = 250 \text{kg/cm}^2$$

The shell element is divided to 3200 elements of dimensions (2.5mm \times 2.5mm)

$$\text{Load per each node} = 250 \times (0.25 \times 0.25) = 15.625 \text{kg}$$

5. Results and analysis:

5.1 Modeling the concrete as a single-phase material:

Figure (2) shows the contour of normal stress S11 of the vertical section passing longitudinal axis of a single phase material. It is clear that modeling the concrete as a single-phase material will not identify the location of failure wherever occurs in the mortar, the aggregate, or at the interface. Table (3) shows the computed normal stress S11 at the longitudinal axis passing the centroid of the vertical plane of the photo where compressive stresses were observed at top and bottom while tensile stresses were observed almost at the middle third of the photo. The tensile stresses ranged from 0.17kg/cm² to 3.63kg/cm².

5.2 Modeling the concrete as a double-phase material (longitudinal section):

The contour of normal stress S11 of the vertical section of concrete modeled as double-phase material is shown in Figures from (3) to (6). The values of normal stress S11 were computed and recorded in Tables (4) and (5).

5.2.1 Effect of modeling procedure:

Table (4) shows the normal stresses S11 at the longitudinal axis passing the centroid of the vertical plane of the photo of mixes contained gravel and compacted either manually or mechanically. The induced stress depends mainly on the phase of the material. The results in Table (4) indicated that the mortar and the interface are subjected to tensile stresses while the aggregates are subjected to compressive stresses. Figure (7) indicated the significant influence of modeling technique on the induced stresses and consequently the structural behavior of the material when exposed to external loads. As shown in Figure (8), modeling the concrete as double-phase material leads to identify the actual stress conditions, tension or compression wherever inside the mortar, the aggregate or at the interface. Similar observations were existed when concerning the mechanically compacted concrete specimen. The difference was in the absolute values of the normal stress S11.

5.2.2 Effect of compaction method on the induced normal stress S11:

As shown in Table (4) of manually compacted concrete mix, the tensile stress S11 induced in the mortar at the middle third ranged from 11.39kg/cm² to

58.80kg/cm². In case of mechanical compaction, the tensile stress S11 in the mortar at the middle third ranged from 8.30kg/cm² to 45.00kg/cm². Similarly, The tensile stress S11 at the interface of the middle third ranged from 13.37kg/cm² to 49.40kg/cm², while it ranged from 5.40kg/cm² to 16.75kg/cm² in case of mechanical compaction. The compressive stress S11 in the aggregate ranged from 29.50kg/cm² to 65.30kg/cm² in case of manual compaction, while it ranged from 5.60kg/cm² to 31.90kg/cm² in case of mechanical compaction. The results in Table (5) show that similar trends were noted for the concrete specimen of mix containing dolomite and the differences were in the absolute values of the normal stress S11. The results indicated that compacted concrete mix using the vibrator leads to induce lower normal stresses when compared to the manually compacted concrete mix.

5.2.3 Effect of aggregate type on the induced normal stress S11:

Figure (7) shows the normal stress S11 at the longitudinal axes passing the planes of the centroid of the photos of mixes contained either gravel or dolomite. The mix that contained gravel showed relatively higher normal stress S11 when compared to that contained dolomite. However, the effect of the type of the aggregate was not clear comparing to the method of compaction. Special treatment of the boundary conditions may be needed to show up the significant effect of the aggregate type. In case of mechanical compaction, the results showed that significant increase in the induced compressive stresses in the gravel aggregates when compared to those induced in the dolomite aggregates. Similar trend was observed in case of the tensile stresses induced in the cement mortar while slight increase in the tensile stresses were observed at the interface of the gravel aggregates when compared to the tensile stresses at the interface of the dolomite aggregates.

5.2.4 Normal stress S11 at the transverse axis of concrete specimen:

Table (6) shows the computed normal stress S11 in the transverse direction through the axis passing the centroid of the photo. The sections are subjected to tensile stresses of minimum value 0.04kg/cm² at the edge and maximum value 2.84kg/cm² at the center. Tables (7) and (8) show the normal stress S11 in the transverse axis passing the centroid of the photo when the concrete is modeled as double phase material. It was clear that relatively higher stress value was obtained for the case of the gravel aggregate when compared to the value of the dolomite aggregate. The mechanically compacted mixes showed relatively smaller normal stress values with respect to the manually compacted mixes. The normal stress values are considered at the middle third of the photo to avoid

the undesirable effect of the boundary conditions at bottom. It has been noticed that the type of the aggregate had a slight effect on the induced normal stress S11 when compared to the effect of the compaction type. This may be due to modeling the interface conditions as a case of fully bonded aggregate to the mortar. However, the finite element analysis succeeded to distinguish between the two aggregate types due to modeling the concrete as double-phase material.

6. Normal stress S11 for sections at top and mid of the photo:

6.1 Modeling the concrete as a single-phase material:

Table (9) and Figure(9) show the normal stress S11 at the vertical and horizontal axes passing the centroid of the photo. The induced tensile stress ranged from 14.66kg/cm² to 19.01kg/cm² and the maximum value has been observed at the center. High compressive stresses are observed at top and bottom. The normal stress S11 at the horizontal section passing the centroid ranged from 0.095 kg/cm² at the edge to 18.99kg/cm² at center. Figure (9) showed that it was impossible to identify the nature of the failure wherever it was in the mortar, at the interface or in the aggregate.

6.2 Modeling the concrete as a double-phase material (circular sections):

6.2.1 Top section for mix contained gravel:

Table (10) and Figures from (10) to (11) show the normal stress S11 at the vertical axis of manually and mechanically compacted specimens respectively. In case of manual compaction, the tensile stress at the middle third ranged from 11.13kg/cm² to 32.56kg/cm² while it ranged from 10.15kg/cm² to 28.03kg/cm² in case of mechanical compaction. Slight reduction in the induced stress S11 was observed in case of mechanical compaction. The maximum tensile stress in the mortar, at the interface, and in the aggregate was 25.75kg/cm² and 24.11kg/cm², and 32.56kg/cm² for the case manual compaction while it was 29.39kg/cm², 21.11kg/cm², and 28.03kg/cm² for the case of mechanical compaction.

The normal stress S11 at the horizontal axis passing the centroid showed that manual compaction led to higher stress with respect to the case of mechanical compaction. Table (11) presents the induced normal stresses in the mortar, the aggregate, and at the interface. For the case of manual compaction the maximum normal stress in the mortar, at the interface, and in the aggregate was 30.33kg/cm², 21.67kg/cm², and 26.11kg/cm² while they were 23.85kg/cm², 26.45kg/cm², and 21.87kg/cm² for the case of mechanical compaction respectively.

6.2.2 Top section of mix contains dolomite:

Table (12) and Figures from (12) to (13) show

the normal stress S_{11} at the top of the vertical sections of manually and mechanically compacted specimens respectively. In case of manual compaction, the tensile stress at the middle third ranged from 19.10kg/cm^2 to 32.90kg/cm^2 while it ranged from 13.11kg/cm^2 to 23.25kg/cm^2 in case of mechanical compaction. Significant reduction in the induced stress S_{11} was observed in case of mechanical compaction. The maximum tensile stress in the mortar was 19.55kg/cm^2 and 19.40kg/cm^2 for manual and mechanical compaction respectively while it was 20.60kg/cm^2 and 23.25kg/cm^2 at the interface.

For the top section, the results of the normal stress S_{11} at the horizontal section passing the centroid show that manual compaction led to higher stress with respect to the case of mechanical compaction. Table (13) shows the induced normal stress in the mortar, aggregate, and at the interface. For the case of manual compaction, the maximum normal stresses in the mortar, at the interface, and the aggregate were 28.72kg/cm^2 , 14.60kg/cm^2 , and 23.44kg/cm^2 while they were 19.45kg/cm^2 , 26.45kg/cm^2 , and 27.75kg/cm^2 for the case of mechanical compaction respectively. Figures (13) and (14) show that the induced stress in case of mechanical compaction was lower than that induced in case of manual compaction.

6.2.3 Mid-section of mix contains gravel:

Table (14) and Figures from (15) to (16) show the normal stress S_{11} of the vertical axis at mid-sections manually and mechanically compacted specimens respectively. In case of manual compaction, the tensile stress at the middle third ranged from 20.95kg/cm^2 to 34.95kg/cm^2 while it ranged from 10.33kg/cm^2 to 26.01kg/cm^2 in case of mechanical compaction. Significant reduction in the induced stress S_{11} was observed in case of mechanical compaction. The maximum tensile stress in the mortar was 34.95kg/cm^2 and 20.44kg/cm^2 for manual and mechanical compaction respectively while it was 24.98kg/cm^2 and 26.01kg/cm^2 at the interface.

For the mid-sections, the results of the normal stress s_{11} at the horizontal axis passing the centroid show that manual compaction led to higher stress with respect to the case of mechanical compaction. Table (15) presents the normal stress induced in the mortar, at the interface, and the in aggregate. For the case of manual compaction the maximum normal stresses in the mortar, at the interface, and in the aggregate were 30.02kg/cm^2 , 25.19kg/cm^2 , and 14.63kg/cm^2 while they were 26.10kg/cm^2 , 18.37kg/cm^2 , and 13.74kg/cm^2 for the case of mechanical compaction respectively.

6.2.4 Mid-section of mix contains dolomite:

Table (16) shows the normal stress S_{11} of the vertical axis at mid-sections of manually and mechanically compacted specimens respectively. In

case of manual compaction, the tensile stress at the middle third ranged from 18.00kg/cm^2 to 32.25kg/cm^2 while it ranged from 13.65kg/cm^2 to 25.33kg/cm^2 in case of mechanical compaction. Significant reduction in the induced stress S_{11} was observed in case of mechanical compaction. The maximum tensile stress in the mortar was 32.25kg/cm^2 and 20.24kg/cm^2 for manual and mechanical compaction respectively while it was 21.27kg/cm^2 and 25.33kg/cm^2 at the interface.

For the mid-sections, the results of the normal stress S_{11} at the horizontal axis passing the centroid show that manual compaction led to higher stress with respect to the case of mechanical compaction. Table (17) presents the normal stress induced in the mortar, at the interface, and the in aggregate. For the case of manual compaction, the maximum normal stresses in the mortar, at the interface, and in the aggregate were 17.57kg/cm^2 , 24.11kg/cm^2 , and 21.60kg/cm^2 while they were 20.22kg/cm^2 , 17.11kg/cm^2 , and 21.75kg/cm^2 for the case of mechanical compaction respectively. Figures (17) and (18) show that the normal stress induced in the dolomite is significantly lower with respect to that induced in the gravel. The observation has been noticed for both manual and mechanical compaction. The same observations have been recorded when concerning the vertical and horizontal sections at the mid-section.

7. Summary and Conclusions:

It is clear from the conducted research work the potential of modeling the material as a multilayer system. Using a single value of the modulus of elasticity which nominated the modulus of elasticity of concrete as input data in the finite element analysis can only predict the induced stresses and strains but it will not lead to specify the location of failure inside the multilayer system. However, the values and distribution of the induced normal stress in case of modeling the concrete as a double-phase material are completely different from the case of modeling it a single-phase material. Identifying the moduli of elasticity of the layers of the system in the finite element analysis by using the DIA technique can establish a new criterion of design by predicting the location of failure. As shown in the conducted research work, the most probable locations of failure were at the interface or in the mortar. This should be further supported by implementing a comprehensive statistical analysis. As verification, the finite element analysis of the photos succeeds to distinguish among the normal stresses S_{11} induced in the concrete specimens of mixes which contained gravel or dolomite aggregate. It also analytically explains the influence of the compaction method in terms of inducing different stresses at the top and mid sections of concrete specimen made of the same concrete mix.

Table 1: Compressive and tensile strength of concrete specimens

Aggregate type	Compaction method	Compressive strength (kg/cm ²)	Tensile strength (kg/cm ²)
Gravel	Manual	250	30
	Mechanical	280	31.7
Dolomite	Manual	300	32.86
	Mechanical	340	34.98

Table 2: Properties of the materials

Property	Gravel	Dolomite	Cement Paste
Mass per unit volume (kg/cm ³)	1.6E-06	1.6E-06	2.4E-06
Wight per unit volume (kg/cm ³)	1.6E-03	1.6E-03	2.4E-03
Modulus of elasticity (kg/cm ²)	5.5E06	5.5E06	2E06
Poisson's ratio	0.15	0.14	0.25
Coefficient of thermal expansion	8.1E-06	8.1E-06	9.9E-06

Table 3: Contour of normal stress (S11) at the longitudinal axis of concrete specimen modeled as a single-phase material

Stress location	Stress (kg/cm ²)	Location	Type
1	-0.660	CEMENT	COMP
2	-0.625	CEMENT	COMP
3	-0.580	CEMENT	COMP
4	-0.530	CEMENT	COMP
5	-0.510	CEMENT	COMP
6	-0.460	CEMENT	COMP
7	-0.360	CEMENT	COMP
8	-0.250	CEMENT	COMP
9	-0.150	CEMENT	COMP
10	-0.100	CEMENT	COMP
11	0.170	CEMENT	TEN
12	0.3500	CEMENT	TEN
13	0.560	CEMENT	TEN
14	0.930	CEMENT	TEN
15	1.230	CEMENT	TEN
16	1.550	CEMENT	TEN
17	1.730	CEMENT	TEN
18	2.280	CEMENT	TEN
19	2.460	CEMENT	TEN
20	2.840	CEMENT	TEN
21	3.020	CEMENT	TEN
22	3.550	CEMENT	TEN
23	3.630	CEMENT	TEN
24	3.580	CEMENT	TEN
25	3.270	CEMENT	TEN
26	2.550	CEMENT	TEN
27	1.300	CEMENT	TEN
28	0.465	CEMENT	TEN
29	-1.900	CEMENT	COMP
30	-3.600	CEMENT	COMP
31	-5.500	CEMENT	COMP
32	-10.400	CEMENT	COMP
33	-20.870	CEMENT	COMP
34	-35.960	CEMENT	COMP
35	-64.080	CEMENT	COMP
36	-72.480	CEMENT	COMP
37	-90.590	CEMENT	COMP
38	-109.960	CEMENT	COMP
39	-129.950	CEMENT	COMP
40	-140.39	CEMENT	COMP

Table 4: Normal stress (S11) at the longitudinal axis of concrete contained gravel and modeled as a double-phase material

tress location	Stress (kg/cm ²)	Location	Type	Stress kg/cm ²	Location	Type
	Manual compaction			Mechanical compaction		
1	115.240	CEMENT	TEN	98.400	SURFACE	TEN
2	-32.040	AGG	COMP	15.300	INTERFACE	TEN
3	-18.020	AGG	COMP	2.200	INTERFACE	TEN
4	20.090	INTERFACE	TEN	-5.600	AGG	COMP
5	40.088	INTERFACE	TEN	17.500	CEMENT	TEN
6	32.190	CEMENT	TEN	-19.000	AGG	COMP
7	12.480	CEMENT	TEN	-14.500	AGG	COMP
8	23.090	CEMENT	TEN	5.900	CEMENT	TEN
9	10.820	CEMENT	TEN	8.500	INTERFACE	TEN
10	9.600	INTERFACE	TEN	-31.900	AGG	COMP
11	-46.000	AGG	COMP	-25.400	AGG	COMP
12	-55.800	AGG	COMP	5.400	INTERFACE	TEN
13	-29.500	AGG	COMP	9.400	CEMENT	TEN
14	29.580	INTERFACE	TEN	15.150	CEMENT	TEN
15	21.5500	CEMENT	TEN	15.110	CEMENT	TEN
16	-12.500	AGG	COM	8.140	INTERFACE	TEN
17	38.150	CEMENT	TEN	8.300	CEMENT	TEN
18	35.630	INTERFACE	TEN	4.190	INTERFACE	TEN
19	-26.900	AGG	COMP	-10.700	AGG	COMP
20	-25.130	AGG	COMP	-7.900	AGG	COMP
21	33.870	CEMENT	TEN	-20.000	AGG	COMP
22	25.170	INTERFACE	TEN	16.750	INTERFACE	TEN
23	25.900	CEMENT	TEN	45.000	CEMENT	TEN
24	11.390	CEMENT	TEN	-14.000	AGG	COM
25	13.370	INTERFACE	TEN	19.890	AGG	TEN
26	-19.880	AGG	COMP	-11.500	AGG	COMP
27	41.700	CEMENT	TEN	10.100	INTERFACE	TEN
28	17.900	CEMENT	TEN	1.800	INTERFACE	TEN
29	49.400	INTERFACE	TEN	-13.700	CEMENT	COMP
30	39.500	INTERFACE	TEN	2.100	CEMENT	TEN
31	58.800	CEMENT	TEN	-80.000	CEMENT	COMP
32	-65.300	AGG	COMP	98.400	SURFACE	TEN
33	19.020	INTERFACE	TEN	15.300	INTERFACE	TEN
34	-4.060	AGG	COMP	2.200	INTERFACE	TEN
35	-106.900	AGG	COMP	-5.600	AGG	COMP
36	-72.400	AGG	COMP	17.500	CEMENT	TEN
37	24.500	INTERFACE	TEN	-19.000	AGG	COMP
38	27.800	INTERFACE	TEN	-14.500	AGG	COMP
39	85.370	CEMENT	TEN	5.900	CEMENT	TEN
40	100.670	CEMENT	TEN	8.500	INTERFACE	TEN

Table 5: Normal stress (S11) at the longitudinal axis of concrete contained dolomite and modeled as a double-phase material

Stress location	Stress (kg/cm ²)	Location	Type	Stress (kg/cm ²)	Location	Type
	Manual compaction			Mechanical compaction		
1	-105.240	AGG	COMP	-94.200	SURFACE	COMP
2	30.110	CEMENT	TEN	12.100	INTERFACE	TEN
3	16.020	INTERFACE	TEN	2.100	AGG	TEN
4	-19.310	AGG	COMP	-3.900	AGG	COMP
5	-36.400	AGG	COMP	15.100	CEMENT	TEN
6	-29.180	AGG	COMP	16.000	CEMENT	TEN
7	9.410	INTERFACE	TEN	-12.300	INTERFACE	COMP
8	20.60	CEMENT	TEN	5.100	AGG	TEN
9	-8.910	AGG	COMP	6.800	INTERFACE	TEN
10	9.100	CEMENT	TEN	22.900	CEMENT	TEN

11	41.000	INTERFACE	TEN	21.400	CEMENT	TEN
12	-51.080	AGG	COMP	-3.900	AGG	COMP
13	22.900	CEMENT	TEN	7.200	INTERFACE	TEN
14	-24.600	AGG	COMP	12.110	CEMENT	TEN
15	19.550	INTERFACE	TEN	13.250	CEMENT	TEN
16	-9.900	AGG	COMP	-7.350	AGG	COMP
17	34.18	INTERFACE	TEN	7.900	CEMENT	TEN
18	30.600	CEMENT	TEN	3.310	INTERFACE	TEN
19	21.900	INTERFACE	TEN	-9.700	AGG	COM
20	-23.400	AGG	COMP	7.100	CEMENT	TEN
21	-31.890	AGG	COMP	18.000	CEMENT	TEN
22	23.970	CEMENT	TEN	-15.310	AGG	COM
23	24.200	INTERFACE	TEN	14.000	INTERFACE	TEN
24	-10.390	AGG	COMP	11.010	CEMENT	TEN
25	-12.950	AGG	COMP	-16.950	AGG	COMP
26	-17.880	AGG	COMP	-9.810	AGG	COMP
27	39.100	INTERFACE	TEN	-9.310	AGG	COMP
28	-15.780	AGG	COMP	1.020	INTERFACE	TEN
29	45.980	CEMENT	TEN	-11.900	AGG	COMP
30	37.050	CEMENT	TEN	2.010	INTERFACE	TEN
31	56.700	INTERFACE	TEN	-23.000	AGG	COMP
32	-63.900	AGG	COMP	61.000	CEMENT	TEN
33	17.050	INTERFACE	TEN	-28.400	AGG	COMP
34	-3.700	AGG	COM	20.100	CEMENT	TEN
35	100.800	INTERFACE	TEN	4.900	CEMENT	TEN
36	-64.600	AGG	COMP	7.200	CEMENT	TEN
37	20.100	CEMENT	TEN	31.200	CEMENT	TEN
38	23.2100	INTERFACE	TEN	40.110	CEMENT	TEN
39	72.990	CEMENT	TEN	31.120	CEMENT	TEN
40	-91.670	AGG	COMP	-60.010	AGG	COMP

Table 6: Contour of normal stress (S11) at the transverse axis of concrete specimen and modeled as a single-phase material

stress location	Stress (kg/cm ²)	Location	Type
1	0.040	CEMENT	TEN
2	0.119	CEMENT	TEN
3	0.410	CEMENT	TEN
4	0.850	CEMENT	TEN
5	1.220	CEMENT	TEN
6	1.520	CEMENT	TEN
7	1.910	CEMENT	TEN
8	2.150	CEMENT	TEN
9	2.660	CEMENT	TEN
10	2.840	CEMENT	TEN
11	2.710	CEMENT	TEN
12	2.630	CEMENT	TEN
13	2.390	CEMENT	TEN
14	1.900	CEMENT	TEN
15	1.520	CEMENT	TEN
16	1.220	CEMENT	TEN
17	0.720	CEMENT	TEN
18	0.370	CEMENT	TEN
19	0.119	CEMENT	TEN
20	0.022	CEMENT	TEN

Table 7: Normal stress (S11) at the transverse axis of concrete contained gravel and modeled as a double-phase material

Stress location	Stress (kg/cm ²)	Location	Type	Stress (kg/cm ²)	Location	Type
	Manual compaction			Mechanical compaction		
1	9.180	CEMENT	TEN	4.900	CEMENT	TEN
2	2.800	INTERFACE	TEN	10.300	CEMENT	TEN
3	-11.700	AGG	COMP	7.900	CEMENT	TEN
4	3.930	INTERFACE	TEN	-9.100	AGG	COMP
5	-23.110	AGG	COM	5.980	INTERFACE	TEN
6	40.100	CEMENT	TEN	-6.200	AGG	COMP
7	49.200	CEMENT	TEN	-20.100	AGG	COMP
8	-18.250	AGG	COMP	-7.900	AGG	COMP
9	-28.400	AGG	COMP	11.350	INTERFACE	TEN
10	21.130	CEMENT	TEN	12.400	CEMENT	TEN
11	17.900	CEMENT	TEN	6.750	CEMENT	TEN
12	23.930	INTERFACE	TEN	7.100	INTERFACE	TEN
13	38.700	CEMENT	TEN	-8.090	AGG	COMP
14	-50.300	AGG	COMP	-11.800	AGG	COMP
15	5.930	CEMENT	TEN	17.900	INTERFACE	TEN
16	-16.900	AGG	COMP	24.900	CEMENT	TEN
17	-20.110	AGG	COMP	-6.950	AGG	COMP
18	15.900	INTERFACE	TEN	16.750	INTERFACE	TEN
19	22.130	CEMENT	TEN	13.390	CEMENT	TEN
20	-14.010	AGG	COMP	12.610	CEMENT	TEN
21	6.350	CEMENT	TEN	3.020	INTERFACE	TEN
22	3.600	CEMENT	TEN	3.600	CEMENT	TEN
23	38.000	CEMENT	TEN	38.000	CEMENT	TEN
24	0.900	CEMENT	TEN	0.900	CEMENT	TEN

Table 8: Normal stress (S11) at the transverse axis of concrete contained dolomite and modeled as a double-phase material

Stress location	Stress (kg/cm ²)	Location	Type	Stress (kg/cm ²)	Location	Type
	Manual compaction			Mechanical compaction		
1	11.800	CEMENT	TEN	6.040	CEMENT	TEN
2	3.900	INTERFACE	TEN	12.000	CEMENT	TEN
3	13.700	INTERFACE	TEN	9.700	CEMENT	TEN
4	5.160	CEMENT	TEN	10.700	CEMENT	TEN
5	-26.500	AGG	COMP	7.160	INTERFACE	TEN
6	66.300	CEMENT	TEN	-7.700	AGG	COMP
7	68.600	CEMENT	TEN	-23.800	AGG	COMP
8	21.500	CEMENT	TEN	9.200	INTERFACE	TEN
9	31.400	INTERFACE	TEN	13.580	INTERFACE	TEN
10	-18.750	AGG	COMP	-13.100	AGG	COMP
11	20.680	CEMENT	TEN	-9.800	AGG	COMP
12	-15.800	AGG	COMP	8.900	INTERFACE	TEN
13	44.200	INTERFACE	TEN	8.140	INTERFACE	TEN
14	39.600	INTERFACE	TEN	13.900	CEMENT	TEN
15	-4.100	AGG	COMP	-20.700	AGG	COMP
16	18.7000	CEMENT	TEN	-28.700	AGG	COMP
17	22.200	CEMENT	TEN	8.300	INTERFACE	TEN
18	-17.060	AGG	COMP	22.300	CEMENT	TEN
19	-24.360	AGG	COMP	-16.700	AGG	COMP
20	15.257	CEMENT	TEN	-15.800	AGG	COMP

Table 9: Normal Stress (S11) at the vertical and horizontal axes of concrete specimen and modeled as a single-phase material

Stress location	Stress (kg/cm ²)	Location	Type	Stress (kg/cm ²)	Location	Type
	Manual compaction			Mechanical compaction		
1	-794.040	CEMENT	COMP	0.095	CEMENT	COMP
2	-28.140	CEMENT	COMP	0.269	CEMENT	COMP
3	14.660	CEMENT	TEN	0.564	CEMENT	TEN
4	17.290	CEMENT	TEN	1.590	CEMENT	TEN
5	17.550	CEMENT	TEN	2.340	CEMENT	TEN
6	17.990	CEMENT	TEN	4.350	CEMENT	TEN
7	18.350	CEMENT	TEN	7.012	CEMENT	TEN
8	18.760	CEMENT	TEN	10.130	CEMENT	TEN
9	18.940	CEMENT	TEN	13.370	CEMENT	TEN
10	18.960	CEMENT	TEN	17.400	CEMENT	TEN
11	18.990	CEMENT	TEN	18.990	CEMENT	TEN
12	19.010	CEMENT	TEN	18.270	CEMENT	TEN
13	18.970	CEMENT	TEN	16.260	CEMENT	TEN
14	18.910	CEMENT	TEN	13.370	CEMENT	TEN
15	18.810	CEMENT	TEN	10.760	CEMENT	TEN
16	18.610	CEMENT	TEN	8.500	CEMENT	TEN
17	18.200	CEMENT	TEN	5.600	CEMENT	TEN
18	17.780	CEMENT	TEN	3.260	CEMENT	TEN
19	16.150	CEMENT	TEN	1.000	CEMENT	TEN
20	-31.460	CEMENT	COMP	0.564	CEMENT	COMP
21	-9.170	CEMENT	COMP	0.269	CEMENT	COMP
22	-795.570	CEMENT	COMP	0.095	CEMENT	COMP

Table 10: Normal Stress (S11) at the vertical axis of concrete contained gravel and modeled as a double-phase material - top section

Stress location	Stress (kg/cm ²)	Location	Type	Stress (kg/cm ²)	Location	Type
	Manual compaction			Mechanical compaction		
1	-923.230	CEMENT	COMP	-889.930	CEMENT	COMP
2	-28.1100	CEMENT	COMP	-20.030	INTERFACE	COMP
3	3.500	AGG	TEN	17.850	AGG	TEN
4	8.120	CEMENT	TEN	14.610	AGG	TEN
5	33.410	AGG	TEN	31.150	CEMENT	TEN
6	17.850	INTERFACE	TEN	15.870	INTERFACE	TEN
7	11.130	CEMENT	TEN	10.150	AGG	TEN
8	17.150	AGG	TEN	20.800	CEMENT	TEN
9	22.960	INTERFACE	TEN	21.110	INTERFACE	TEN
10	32.560	AGG	TEN	28.030	AGG	TEN
11	25.750	CEMENT	TEN	23.850	CEMENT	TEN
12	21.410	INTERFACE	TEN	20.150	INTERFACE	TEN
13	29.390	INTERFACE	TEN	19.970	AGG	TEN
14	26.530	AGG	TEN	25.780	AGG	TEN
15	19.610	INTERFACE	TEN	24.110	CEMENT	TEN
16	47.110	AGG	TEN	45.320	INTERFACE	TEN
17	16.840	AGG	TEN	20.200	AGG	TEN
18	1.120	CEMENT	TEN	11.220	CEMENT	TEN
19	6.800	CEMENT	TEN	8.150	CEMENT	TEN
20	-32.890	CEMENT	COMP	-36.000	INTERFACE	COMP
21	-141.160	CEMENT	COMP	-140.1100	AGG	COMP
22	-1099.130	CEMENT	COMP	-1100.120	CEMENT	COMP

Table 11: Normal Stress (S11) at the horizontal axis of concrete contained gravel and modeled as a double-phase material- top section

Stress location	Stress (kg/cm ²)	Location	Type	Stress (kg/cm ²)	Location	Type
	Manual compaction			Mechanical compaction		
1	0.079	CEMENT	TEN	0.051	CEMENT	TEN
2	0.350	CEMENT	TEN	0.280	CEMENT	TEN
3	0.580	CEMENT	TEN	0.420	INTERFACE	TEN
4	1.090	INTERFACE	TEN	0.980	AGG	TEN
5	3.340	AGG	TEN	2.860	AGG	TEN
6	5.370	AGG	TEN	4.910	CEMENT	TEN
7	10.220	CEMENT	TEN	9.120	INTERFACE	TEN
8	13.010	INTERFACE	TEN	12.310	AGG	TEN
9	21.670	INTERFACE	TEN	21.000	CEMENT	TEN
10	30.330	CEMENT	TEN	29.650	AGG	TEN
11	28.790	CEMENT	TEN	23.850	CEMENT	TEN
12	29.210	CEMENT	TEN	26.450	INTERFACE	TEN
13	26.110	AGG	TEN	21.870	AGG	TEN
14	14.090	INTERFACE	TEN	14.250	AGG	TEN
15	15.890	AGG	TEN	13.250	CEMENT	TEN
16	9.440	INTERFACE	TEN	10.110	INTERFACE	TEN
17	10.100	CEMENT	TEN	8.220	AGG	TEN
18	2.890	CEMENT	TEN	1.060	INTERFACE	TEN
19	4.960	INTERFACE	TEN	2.630	CEMENT	TEN
20	0.830	AGG	TEN	4.090	CEMENT	TEN
21	0.240	AGG	TEN	0.610	CEMENT	TEN
22	0.099	CEMENT	TEN	0.041	CEMENT	TEN

Table 12: Normal stress (S11) at the vertical axis of concrete contained dolomite and modeled as a double-phase material- top section

Stress location	Stress (kg/cm ²)	Location	Type	Stress (kg/cm ²)	Location	Type
	Manual compaction			Mechanical compaction		
1	-818.000	CEMENT	COMP	-802.5	CEMENT	COMP
2	-32.200	CEMENT	COMP	-15.45	CEMENT	COMP
3	18.100	CEMENT	TEN	19.8	INTERFACE	TEN
4	27.120	INTERFACE	TEN	15.6	AGGREGATE	TEN
5	19.260	CEMENT	TEN	9.06	INTERFACE	TEN
6	16.970	INTERFACE	TEN	16.09	AGGREGATE	TEN
7	20.130	AGGREGATE	TEN	13.11	AGGREGATE	TEN
8	32.900	AGGREGATE	TEN	13.65	INTERFACE	TEN
9	19.550	CEMENT	TEN	18.15	CEMENT	TEN
10	19.100	CEMENT	TEN	16.4	INTERFACE	TEN
11	19.690	AGGREGATE	TEN	17.45	CEMENT	TEN
12	24.600	AGGREGATE	TEN	19.4	CEMENT	TEN
13	23.980	AGGREGATE	TEN	21.2	AGGREGATE	TEN
14	20.600	INTERFACE	TEN	23.25	INTERFACE	TEN
15	19.590	INTERFACE	TEN	18.1	CEMENT	TEN
16	20.330	AGGREGATE	TEN	40.6	CEMENT	TEN
17	15.040	CEMENT	TEN	18.1	INTERFACE	TEN
18	2.300	AGGREGATE	TEN	10.1	CEMENT	TEN
19	1.700	INTERFACE	TEN	6.71	INTERFACE	TEN
20	-25.250	CEMENT	COMP	-31	CEMENT	COMP
21	-122.070	CEMENT	COMP	-130.2	CEMENT	COMP
22	-787.860	CEMENT	COMP	-974.1	CEMENT	COMP

Table13: Normal stress (S11) at the horizontal axis of concrete contained dolomite and modeled as a double-phase material- top section

Stress location	Stress (kg/cm ²)	Location	Type	Stress (kg/cm ²)	Location	Type
	Manual compaction			Mechanical compaction		
1	0.032	CEMENT	TEN	0.040	CEMENT	TEN
2	0.031	INTERFACE	TEN	0.210	CEMENT	TEN
3	0.048	CEMENT	TEN	0.310	CEMENT	TEN
4	0.910	AGGREGATE	TEN	0.950	INTERFACE	TEN
5	3.100	AGGREGATE	TEN	2.400	AGGREGATE	TEN
6	4.290	CEMENT	TEN	3.850	AGGREGATE	TEN
7	9.140	INTERFACE	TEN	8.150	CEMENT	TEN
8	12.750	CEMENT	TEN	11.400	INTERFACE	TEN
9	19.100	AGGREGATE	TEN	20.300	AGGREGATE	TEN
10	23.440	AGGREGATE	TEN	27.750	AGGREGATE	TEN
11	21.010	CEMENT	TEN	19.450	CEMENT	TEN
12	28.720	CEMENT	TEN	24.650	INTERFACE	TEN
13	22.450	CEMENT	TEN	18.130	AGGREGATE	TEN
14	14.600	INTERFACE	TEN	12.400	AGGREGATE	TEN
15	11.870	AGGREGATE	TEN	11.400	CEMENT	TEN
16	4.430	CEMENT	TEN	9.070	INTERFACE	TEN
17	2.600	AGGREGATE	TEN	5.430	CEMENT	TEN
18	1.000	INTERFACE	TEN	0.980	AGGREGATE	TEN
19	2.700	AGGREGATE	TEN	2.400	AGGREGATE	TEN
20	0.700	INTERFACE	TEN	3.850	CEMENT	TEN
21	0.150	CEMENT	TEN	0.230	CEMENT	TEN
22	0.083	CEMENT	TEN	0.039	CEMENT	TEN

Table 14: Normal stress (S11) at the vertical axis of concrete contained gravel and modeled as a double-phase material - mid section

Stress location	Stress (kg/cm ²)	Location	Type	Stress (kg/cm ²)	Location	Type
	Manual compaction			Mechanical compaction		
1	-950.12	CEMENT	COMP	-818.400	CEMENT	COMP
2	-33.780	CEMENT	COMP	-16.400	INTERFACE	COMP
3	23.600	INTERFACE	TEN	17.260	CEMENT	TEN
4	17.920	AGG	TEN	23.940	AGG	TEN
5	38.170	AGG	TEN	14.690	INTERFACE	TEN
6	18.650	INTERFACE	TEN	15.560	AGG	TEN
7	10.830	INTERFACE	TEN	18.730	INTERFACE	TEN
8	20.950	CEMENT	TEN	20.350	CEMENT	TEN
9	24.620	AGG	TEN	18.110	INTERFACE	TEN
10	34.950	CEMENT	TEN	10.330	CEMENT	TEN
11	28.790	CEMENT	TEN	20.440	CEMENT	TEN
12	27.830	CEMENT	TEN	25.750	INTERFACE	TEN
13	23.160	INTERFACE	TEN	23.350	AGG	TEN
14	29.170	CEMENT	TEN	22.710	CEMENT	TEN
15	24.980	INTERFACE	TEN	26.010	INTERFACE	TEN
16	47.370	AGG	TEN	37.650	CEMENT	TEN
17	20.720	CEMENT	TEN	19.600	AGG	TEN
18	1.600	INTERFACE	TEN	14.800	CEMENT	TEN
19	7.640	CEMENT	TEN	5.300	INTERFACE	TEN
20	-36.900	CEMENT	COMP	-32.000	AGG	COMP
21	-145.950	CEMENT	COMP	-120.290	CEMENT	COMP
22	-1130.750	CEMENT	COMP	-516.180	CEMENT	COMP

Table 15: Normal stress (S11) at the horizontal axis of concrete contained gravel and modeled as a double-phase material - mid section

Stress location	Stress (kg/cm ²)	Location	Type	Stress (kg/cm ²)	Location	Type
	Manual compaction			Mechanical compaction		
1	0.098	CEMENT	TEN	0.049	CEMENT	TEN
2	0.310	CEMENT	TEN	0.015	CEMENT	TEN
3	0.500	INTERFACE	TEN	0.040	INTERFACE	TEN
4	0.950	AGG	TEN	0.900	AGG	TEN
5	2.950	AGG	TEN	2.300	CEMENT	TEN
6	5.090	CEMENT	TEN	3.950	CEMENT	TEN
7	8.810	INTERFACE	TEN	7.130	INTERFACE	TEN
8	11.990	AGG	TEN	12.300	AGG	TEN
9	19.800	INTERFACE	TEN	16.500	CEMENT	TEN
10	30.020	CEMENT	TEN	26.100	CEMENT	TEN
11	25.750	CEMENT	TEN	20.440	CEMENT	TEN
12	29.000	CEMENT	TEN	22.850	CEMENT	TEN
13	25.190	INTERFACE	TEN	18.370	INTERFACE	TEN
14	12.090	AGG	TEN	13.740	AGG	TEN
15	14.630	AGG	TEN	10.390	AGG	TEN
16	8.310	INTERFACE	TEN	7.950	CEMENT	TEN
17	10.300	CEMENT	TEN	0.809	CEMENT	TEN
18	1.950	CEMENT	TEN	0.915	CEMENT	TEN
19	4.110	AGG	TEN	3.040	INTERFACE	TEN
20	0.710	INTERFACE	TEN	0.325	CEMENT	TEN
21	0.160	CEMENT	TEN	0.140	CEMENT	TEN
22	0.088	CEMENT	TEN	0.018	CEMENT	TEN

Table 16: Normal stress (S11) at the vertical axis of concrete contained dolomite and modeled as a double-phase material - mid section

Stress location	Stress (kg/cm ²)	Location	Type	Stress (kg/cm ²)	Location	Type
	Manual compaction			Mechanical compaction		
1	-904.310	CEMENT	COMP	-711.600	CEMENT	COMP
2	-29.800	CEMENT	COMP	-13.280	CEMENT	COMP
3	19.350	INTERFACE	TEN	15.330	CEMENT	TEN
4	11.310	CEMENT	TEN	21.620	INTERFACE	TEN
5	29.320	CEMENT	TEN	12.600	AGG	TEN
6	16.150	AGGREGATE	TEN	14.380	AGG	TEN
7	8.900	INTERFACE	TEN	16.680	INTERFACE	TEN
8	18.000	AGGREGATE	TEN	20.240	CEMENT	TEN
9	21.270	INTERFACE	TEN	17.100	CEMENT	TEN
10	32.250	CEMENT	TEN	13.650	INTERFACE	TEN
11	21.010	CEMENT	TEN	16.150	CEMENT	TEN
12	23.440	AGGREGATE	TEN	22.980	INTERFACE	TEN
13	18.030	CEMENT	TEN	21.380	AGG	TEN
14	22.650	CEMENT	TEN	20.110	INTERFACE	TEN
15	21.900	INTERFACE	TEN	25.330	INTERFACE	TEN
16	46.950	CEMENT	TEN	35.440	CEMENT	TEN
17	15.140	CEMENT	TEN	16.400	AGG	TEN
18	1.700	AGGREGATE	TEN	12.370	CEMENT	TEN
19	4.600	AGGREGATE	TEN	4.740	INTERFACE	TEN
20	-36.120	CEMENT	COMP	-29.000	AGG	COMP
21	-125.580	CEMENT	COMP	-112.970	CEMENT	COMP
22	-1074.380	CEMENT	COMP	-601.500	CEMENT	COMP

Table 17: Normal stress (S11) at the horizontal axis of concrete contained dolomite and modeled as a double-phase material - mid section

Stress location	Stress (kg/cm ²)	Location	Type	Stress (kg/cm ²)	Location	Type
	Manual compaction			Mechanical compaction		
1	0.018	CEMENT	TEN	0.040	CEMENT	TEN
2	0.250	CEMENT	TEN	0.190	CEMENT	TEN
3	0.430	INTERFACE	TEN	0.490	INTERFACE	TEN
4	1.020	AGGREGATE	TEN	0.830	AGGREGATE	TEN
5	2.160	CEMENT	TEN	2.100	CEMENT	TEN
6	6.190	CEMENT	TEN	5.060	CEMENT	TEN
7	9.660	CEMENT	TEN	6.750	INTERFACE	TEN
8	13.400	INTERFACE	TEN	11.100	INTERFACE	TEN
9	18.570	INTERFACE	TEN	15.400	CEMENT	TEN
10	19.780	INTERFACE	TEN	18.330	CEMENT	TEN
11	21.600	AGGREGATE	TEN	20.215	CEMENT	TEN
12	24.110	INTERFACE	TEN	21.750	AGGREGATE	TEN
13	17.570	CEMENT	TEN	17.110	INTERFACE	TEN
14	15.010	CEMENT	TEN	13.970	AGGREGATE	TEN
15	12.910	INTERFACE	TEN	11.970	INTERFACE	TEN
16	10.240	AGGREGATE	TEN	8.450	CEMENT	TEN
17	6.750	CEMENT	TEN	6.100	CEMENT	TEN
18	5.210	INTERFACE	TEN	4.816	INTERFACE	TEN
19	4.200	AGGREGATE	TEN	2.900	INTERFACE	TEN
20	1.090	AGGREGATE	TEN	0.650	CEMENT	TEN
21	0.680	CEMENT	TEN	0.310	CEMENT	TEN
22	0.015	CEMENT	TEN	0.010	CEMENT	TEN



Photo (1): Preparing the longitudinal sections



Photo (2): Preparing the horizontal sections

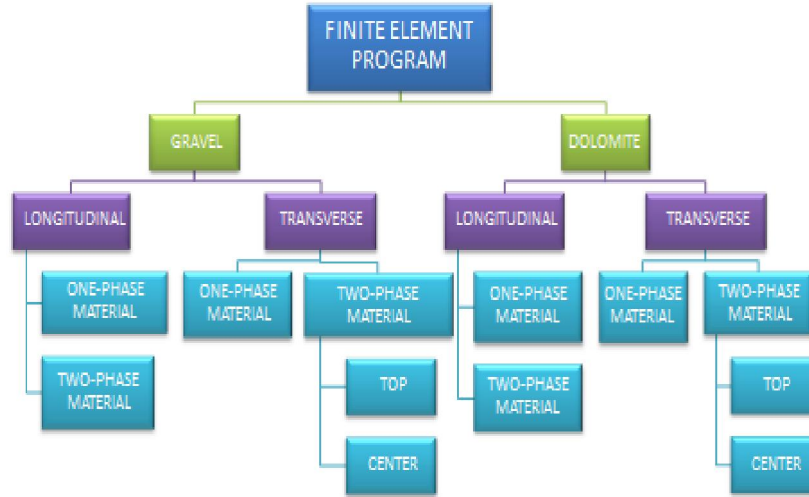


Photo (3): The finite element program

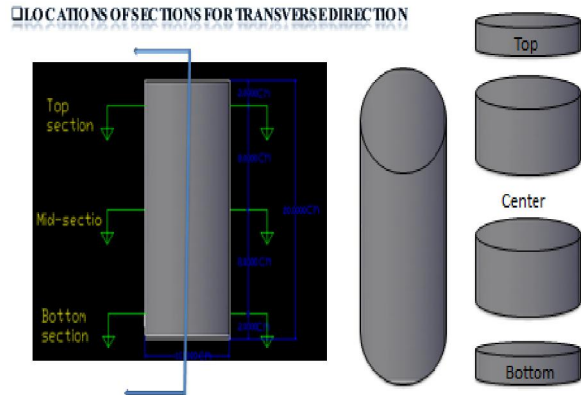


Figure (1): Longitudinal and horizontal circular sections photographed by digital camera

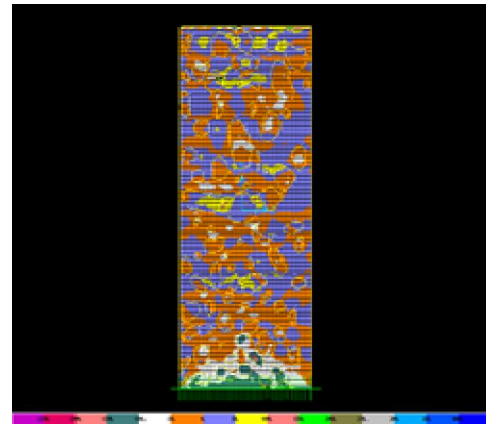


Figure (3): Contour of normal stress S11 of concrete specimen contained gravel and modeled as a double-phase material (Manual compaction)

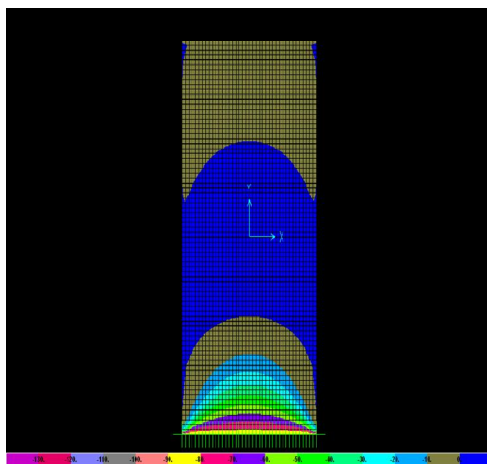


Figure (2): Contour of normal stress S11 of concrete specimen modeled as a single phase-material

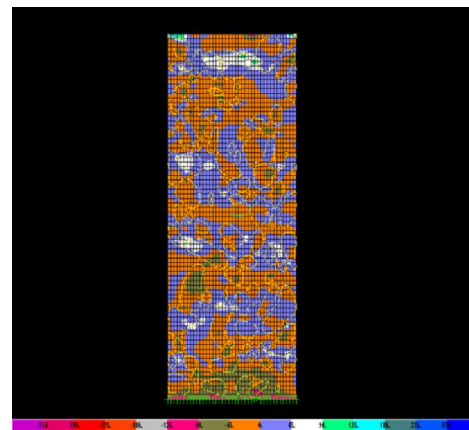


Figure (4): Contour of normal stress S11 of concrete specimen contained gravel and modeled as a double-phase material (Mechanical compaction)

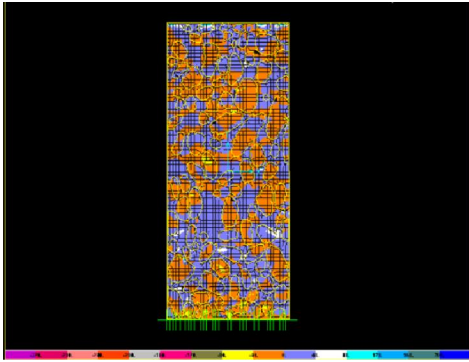


Figure (5): Contour of normal stress S11 of concrete specimen contained dolomite and modeled as a double-phase material(Manual compaction)

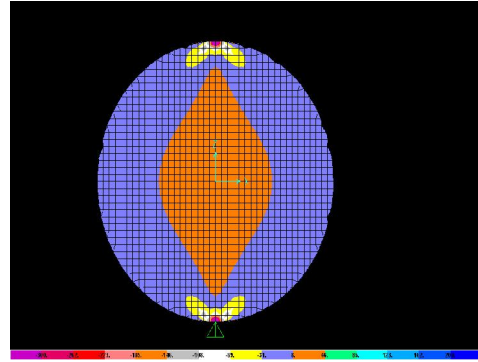


Figure (9): Contour of normal stress (S11) of concrete specimen modeled as a single-phase material

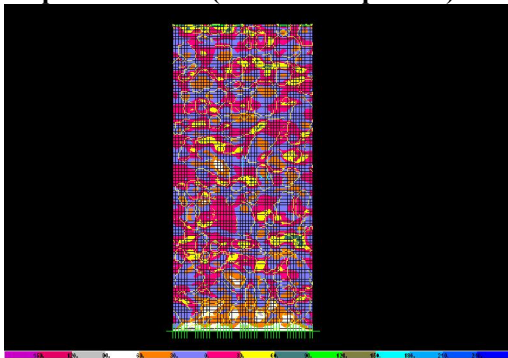


Figure (6): Contour of normal stress S11 of concrete specimen contained dolomite and modeled as a double-phase material (Mechanical compaction)

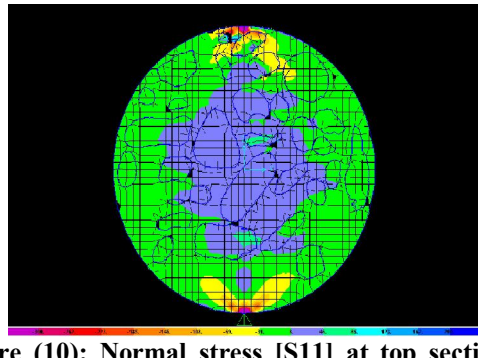


Figure (10): Normal stress [S11] at top section of concrete contained gravel and compacted manually

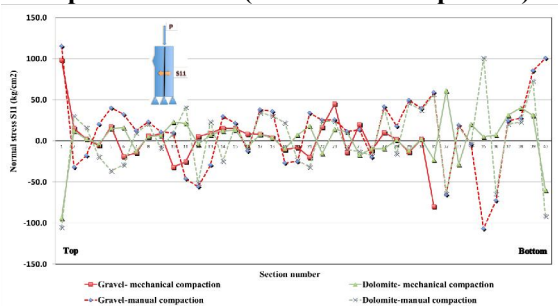


Figure (7): Normal stress S11 at the longitudinal axis of concrete contained gravel and dolomite (Manual and mechanical compaction)

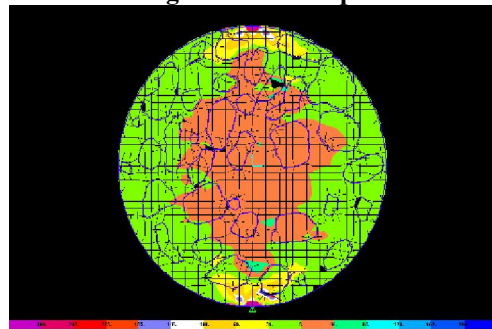


Figure (11): Normal Stress [S11] at top section of concrete contained gravel and compacted mechanically

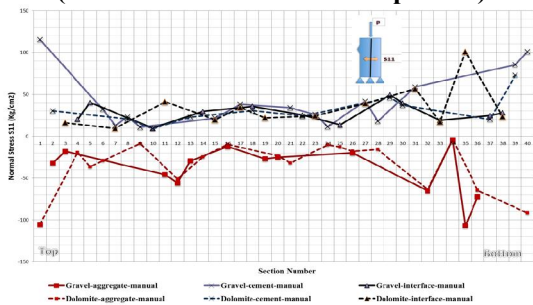


Figure (8): Normal Stress S11 at the different Phases at the longitudinal axis of concrete contained gravel and dolomite (Manual and mechanical compaction)

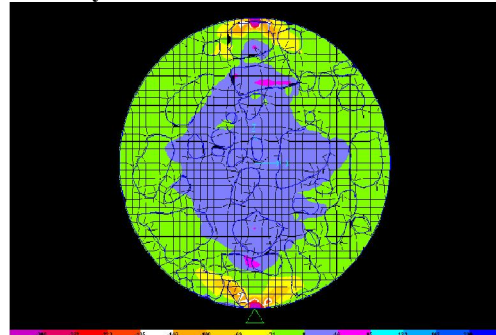


Figure (12): Normal stress [S11] at top section of concrete contained dolomite and compacted manually

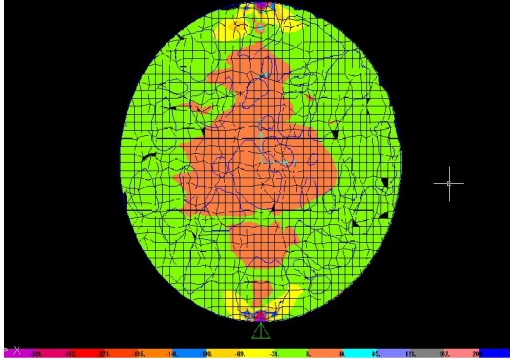


Figure (13): Normal stress [S11] at top section of concrete contained dolomite and compacted mechanically

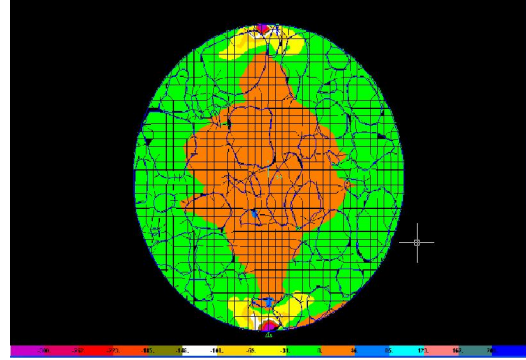


Figure (15): Normal stress [S11] at center section of concrete contained gravel and compacted mechanically

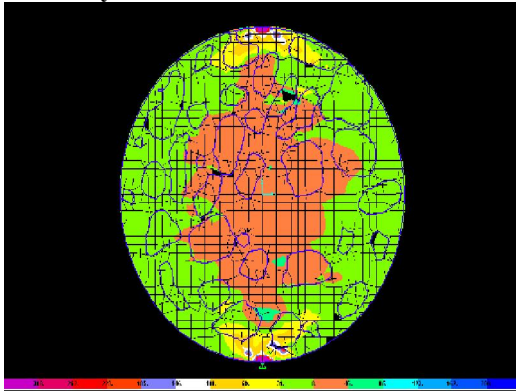


Figure (14): Normal stress [S11] at center section of concrete contained gravel and compacted manually

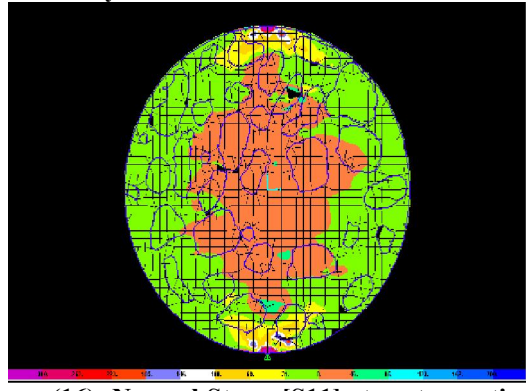
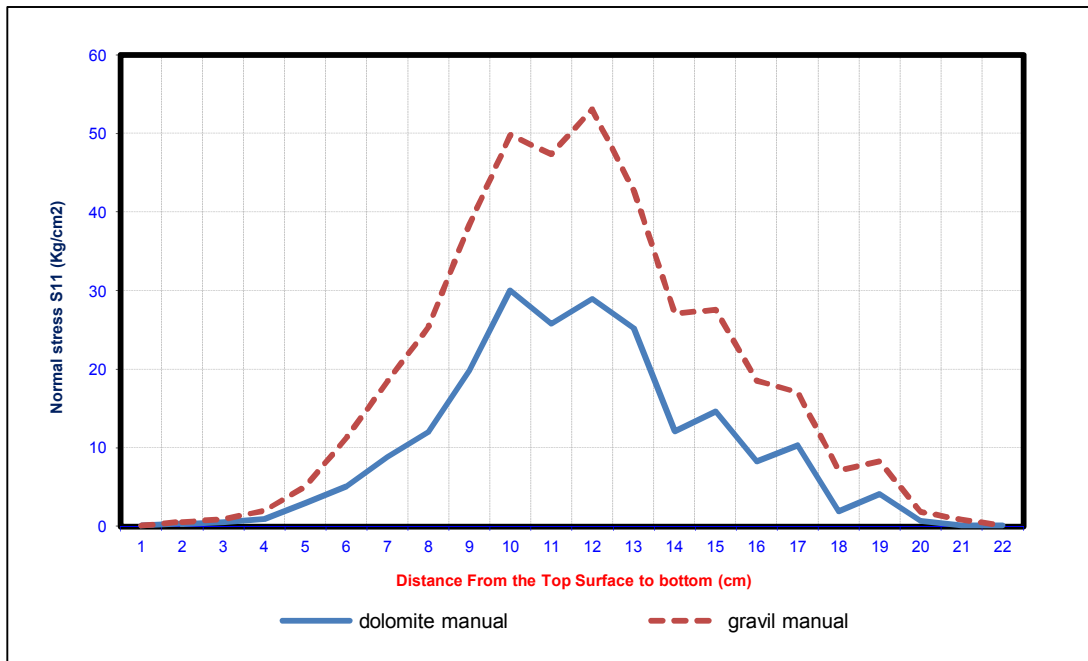


Figure (16): Normal Stress [S11] at center section of concrete contained dolomite and compacted manually



Figure(17): Normal stress (S11) at the horizontal axes of center sections of concrete contained gravel and dolomite aggregate - (Manual compaction)

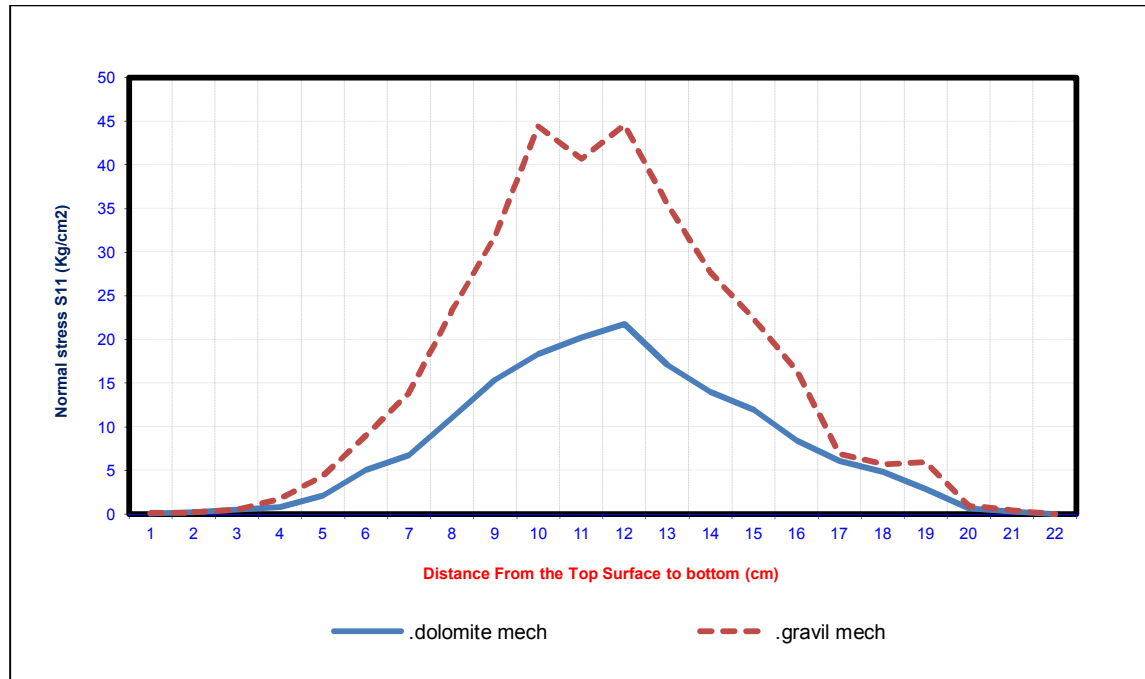


Figure (18): Normal stress (S11) at the horizontal axes of center sections of concrete contained gravel and dolomite aggregate - (Mechanical compaction)

References:

1. Wittmann, F.E. (Ed.), "Fracture Toughness and Fracture Energy of Concrete", Elsevier science Publishers, Amsterdam, 1983.
2. Chen, C.T. and Chen, W.F., "Concrete in Biaxial Cyclic Compression", Journal of Structural Engineering Division, ASCE, VOL. 101, NO.4, PP.461-476, 1975.
3. Chen, W.F., "Plasticity in Reinforced Concrete", McGraw-Hill, New York, 1982.
4. Tanabe, T. and Wu, z., "An Application of Work Hardening and Strain Softening Plasticity to Uniformly Cracked Reinforced Concrete Elements", proc. Of the Third International Conference on Computational Plasticity, Fundamental and Application, pine ridge press, Swansea, UK, pp. 705-716, 1992.
5. Yang, B.L., Dafalias, Y.F. and Herrmann, L.R., "A Bounding Surface Plasticity Model for Concrete", Journal of Engineering Mechanics Division, ASCE, Vol.111, No.3, pp.359-380, 1985.
6. Kotsovos, M.D. and Newman, J.B, "Generalized Stress- Strain Relations for Concrete", Journal of Engineering Mechanics Division, ASCE, Vol. 104, No.4, pp.845-856, 1978.
7. Dougill, J. W., "On Stable Progressively Fracturing Solids", Journal of Applies Mathematics and Physics (ZAMP), Vol.27, pp.423-436, 1976.
8. Hans, D.J. AND Chen, W.F., "Strain Space Plasticity Formulation for Hardening Softening Materials with Elasto-plastic Coupling ", Journal of Solids and Structures, Vol. 22, No. 8, pp.935-950, 1986.
9. Bazant, z.p. and Kim, s., "Plastic-Fracturing Theory for Concrete", Journal of Engineering Mechanics Division, ASCE, Vol.105, No.3, pp.407-428, 1979.
10. Megure, k. and Hakuno, M., "Fracture Analysis of Concrete Structures by the Distinct Element Method", proc. of the Japan Society of Civil Engineers, JSCE. No. 410/I-12, pp 283-294, 1989.

12/2/2013